

INFRARED SPECTRA OF CRYSTALLINE PHASE ICES CONDENSED ON SILICATE SMOKES AT $T < 20$ K

MARLA H. MOORE,¹ ROBERT F. FERRANTE,² REGGIE L. HUDSON,³ JOSEPH A. NUTH III,¹ AND BERTRAM DONN^{1,4}
 Astrochemistry Branch, Laboratory for Extraterrestrial Physics, NASA/Goddard Space Flight Center, Greenbelt, MD 20771

Received 1993 November 12; accepted 1994 April 4

ABSTRACT

Infrared spectra of H₂O, CH₃OH, and NH₃ condensed at $T < 20$ K on amorphous silicate smokes reveal that predominantly crystalline phase ice forms directly on deposit. Spectra of these molecules condensed on aluminum substrates at $T < 20$ K indicate that amorphous phase ice forms. On aluminum, crystalline phase H₂O and CH₃OH are formed by annealing amorphous deposits to 155 K and 130 K, respectively (or by direct deposit at these temperatures); crystalline NH₃ is formed by direct deposit at 88 K. Silicate smokes are deposited onto aluminum substrates by evaporation of SiO solid or by combustion of SiH₄ with O₂ in flowing H₂ followed by vapor phase nucleation and growth. Silicate smokes which are oxygen-deficient may contain active surface sites which facilitate the amorphous-to-crystalline phase transition during condensation. Detailed experiments to understand the mechanism are currently in progress. The assumption that amorphous phase ice forms routinely on grains at $T < 80$ K is often used in models describing the volatile content of comets or in interpretations of interstellar cloud temperatures. This assumption needs to be reexamined in view of these results.

Subject headings: comets: general — dust, extinction — infrared: general — ISM: molecules —
 line: identification — techniques: spectroscopic

Comets are believed to have formed from grains and amorphous ices located in the outer part of the presolar nebula 4.6×10^9 yr ago or in interstellar clouds (for a review see Donn 1991). Based on the interstellar dust model of Greenberg (1982), individual grains are likely to contain a silicate core, a mantle of refractory material, and an outer layer of H₂O dominated volatile ices. The signature of these ice/dust materials is often detected in comets and in interstellar objects. For example, the 9.7 μ m feature attributed to silicates is observed in a variety of interstellar sources (e.g., Nuth & Hecht 1990) and has been observed in several comets (e.g., Bregman et al. 1987). The mid-infrared features of H₂O have been detected in more than 50 sources. Frequently the 3 μ m region of interstellar sources is fitted with laboratory spectra of amorphous phase water ice or water-rich icy mixtures (e.g., Smith, Sellgren, & Tokunaga 1989). However, fitting the band shape sometimes requires both the amorphous and crystalline phase of H₂O even when a mixture of other components is used.

The formation of amorphous phase deposits of H₂O and many other volatile species at $T < 50$ K is documented in numerous laboratory studies using X-ray techniques (e.g., Narten, Venkatesh, & Rice 1976). Amorphous ice, once formed, is unstable against temperature cycling. It converts irreversibly to a crystalline phase on a timescale which decreases with increasing temperature. The conversion is completed on the order of minutes, for example, for H₂O at 155 K and for CH₃OH at 130 K.

Laboratory measurements of various ice/dust properties are crucial for our understanding of these complex comet mixtures (Boice, Naegeli, & Hubner 1989) and interstellar analogs. Zhao

(1990) compared a residue formed from a photolyzed icy mixture on a pressed silicate powder (ground from bulk materials to a grain size near 100s of nanometers) with a residue from a photolyzed icy mixture deposited on a metal substrate. He detected some changes in the subfeatures in the 3.4 μ m absorption region and in the rate of formation of —NH₂ groups. The idea that very reactive surface sites can form in high surface area SiO₂ powders has been studied using gas phase reactions of interest to the microelectronics industry; for example, the dissociation of NH₃ and H₂O during chemisorption has been documented (Morrow & Cody 1976). Similar studies of ice/silicate mixtures have not been done.

In this *Letter* we report on laboratory studies showing that predominantly crystalline phase ices form at $T < 20$ K on laboratory-produced silicate smokes. Infrared spectra of H₂O, CH₃OH, and NH₃ are discussed; SO₂ and H₂CO have also been studied with similar results. H₂O and CH₃OH are abundant interstellar molecules and play important roles in the physical chemistry of comets; NH₃ may play a less important role.

Silicate smokes were made either by evaporation of SiO solid (Nuth & Donn 1982) or by combustion of SiH₄ with O₂ followed by vapor phase nucleation and growth in an H₂ atmosphere (Nelson et al. 1989). Smokes were deposited onto polished aluminum substrates (area = 5 cm²); thicknesses were typically 0.1–0.5 mm. Smoke colors were shades of beige-gold indicating an oxygen-deficient silicate; completely oxidized silicate (SiO₂) is white. Smoke particles are typically 5–10 nm in diameter (Rietmeijer & Nuth 1991) and are generally amorphous in composition and in morphology (Rietmeijer, Nuth, & MacKinnon 1986); individual smoke grains consolidate during deposition resulting in a smoke porosity we estimate to be 97%. Bonding to the aluminum was not a problem, although the smokes were fragile and could easily be compressed or rubbed off. All samples were stored in a vacuum desiccator until used for an experiment. Preliminary measure-

¹ Postal address: NASA/GSFC, Code 691, Greenbelt, MD 20771.

² NASA/GSFC Visiting Summer Fellow. Postal address: US Naval Academy, Chemistry Department, 572 Holloway Road, Annapolis, MD 21402.

³ Postal address: Department of Chemistry, Eckerd College, St. Petersburg, FL 33733.

⁴ Also University of Virginia, Charlottesville. USRA Visiting Scientist.

ments yield a typical smoke density of 0.08 g cm^{-3} ; the surface area of these smokes, determined from N_2 adsorption isotherms at 77 K , is $\sim 125 \text{ m}^2 \text{ g}^{-1}$.

The absorbance spectrum of a typical oxygen-deficient silicate smoke is shown in Figure 1 from 1600 cm^{-1} ($6.2 \text{ }\mu\text{m}$) to 400 cm^{-1} ($25 \text{ }\mu\text{m}$), a region which contains the strongest absorption bands (absorptions in other regions are very weak or nonexistent). Characteristic absorptions of both amorphous SiO_2 and Si_2O_3 are present (Nuth & Donn 1982). The so-called $10 \text{ }\mu\text{m}$ silicate feature peaks at 1087 cm^{-1} ($9.2 \text{ }\mu\text{m}$); less intense bands occur at 880 cm^{-1} ($11.4 \text{ }\mu\text{m}$) and 457 cm^{-1} ($21.9 \text{ }\mu\text{m}$). In contrast to this spectral profile, highly oxidized silicate smokes have strong absorptions at 808 cm^{-1} ($12.4 \text{ }\mu\text{m}$) and near 460 cm^{-1} ($21.6 \text{ }\mu\text{m}$).

Each ice/silicate composite was formed in vacuum by slow condensation of gas onto a silicate smoke which was cooled to $T < 20 \text{ K}$. The rate of deposition was the order of 10^{20} molecules hr^{-1} which is equivalent to ~ 10 s of microns hr^{-1} on an aluminum substrate, but is estimated to be only ~ 10 s of monolayers hr^{-1} on each grain of a 0.5 mm thick smoke. Since ice/silicate spectra were compared to ice spectra on aluminum substrates, typical minimum absorbances for a $\text{CH}_3\text{OH}/\text{silicate}$ in the $3 \text{ }\mu\text{m}$ region were 0.2. These deposits routinely formed crystalline ices. Ultrathin CH_3OH deposits (absorbance < 0.2) on silicates were amorphous but evolved, with the addition of more CH_3OH at $T < 20 \text{ K}$, into the crystalline signatures we originally observed. We estimate the transition to the crystalline ices occurs after the equivalent of ≈ 10 monolayers of condensate have formed. Spectra of the $45 \text{ }\mu\text{m}$ band of H_2O , the $3 \text{ }\mu\text{m}$ region of CH_3OH , and the $10 \text{ }\mu\text{m}$ region of NH_3 were recorded using a Mattson (Polaris) FTIR. These spectral regions were chosen because of the large differences observed between the amorphous and crystalline spectral profiles. Spectra consist of at least 60 coadded scans and have a resolution of 4 cm^{-1} . In our configuration, the infrared beam is reflected from the aluminum substrate producing an

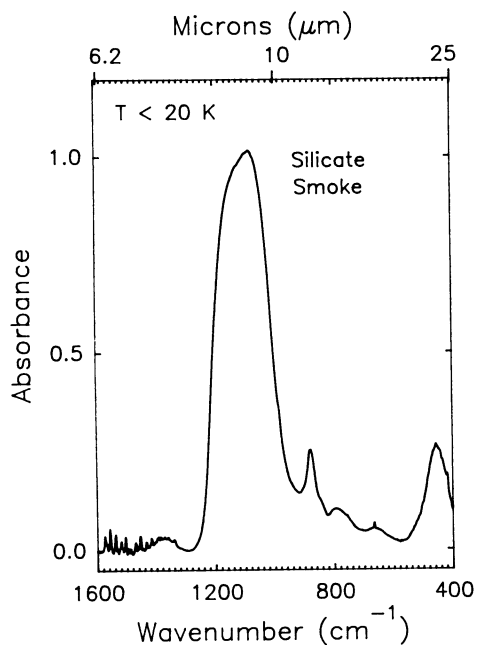


FIG. 1.—Infrared spectrum, typical of laboratory-produced silicate smokes on aluminum substrate, is a mixture of SiO_2 and Si_2O_3 .

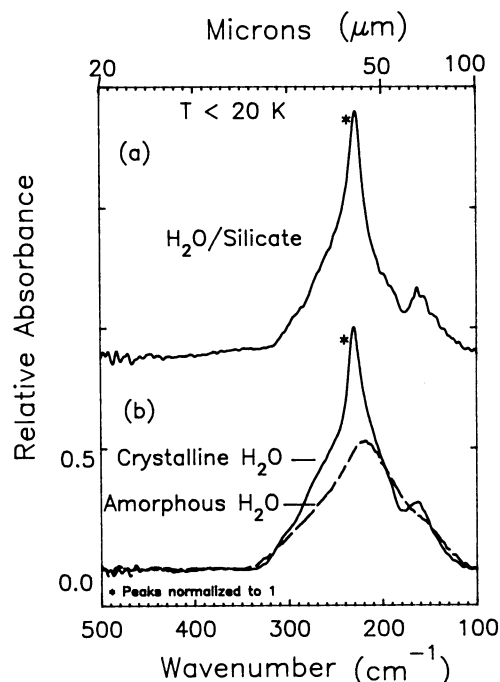


FIG. 2.—Far-infrared spectra of H_2O . H_2O deposited directly onto a silicate smoke (a) is compared with spectra of H_2O in the amorphous and crystalline phase on an aluminum substrate (b).

absorbance spectrum after two passes through the ice/silicate film. Each ice/silicate spectrum was ratioed with the spectrum of the pure silicate to remove the silicate features from the spectrum (for more details, see Moore & Hudson 1992).

Figure 2 summarizes the far-infrared spectral results for H_2O deposits at $T < 20 \text{ K}$. H_2O condensed onto silicate smoke results in the $\text{H}_2\text{O}/\text{silicate}$ spectrum shown in Figure 2a. This spectrum is compared with Figure 2b showing the single broad symmetrical band of amorphous ice deposited on an aluminum substrate at $T < 20 \text{ K}$ ⁵ and the spectrum of that same ice converted to the crystalline form by warming to 155 K and then recoiling to 13 K . The ice/silicate bands at 230 cm^{-1} ($43.5 \text{ }\mu\text{m}$) and 162 cm^{-1} ($61.7 \text{ }\mu\text{m}$) correspond to the assigned positions for the transverse optical and longitudinal acoustic modes of crystalline H_2O , respectively (Bertie, Labbé, & Whalley 1969). The $\text{H}_2\text{O}/\text{silicate}$ spectrum is best fitted with the spectrum of crystalline H_2O on aluminum. The addition of an amorphous ice component broadens the spectrum resulting in a poorer fit.

Figure 3 shows the results for CH_3OH deposits in the O—H stretch region at $T < 20 \text{ K}$. Figure 3a is the spectrum of $\text{CH}_3\text{OH}/\text{silicate}$. This is compared in Figure 3b with the broad band typical of amorphous phase CH_3OH deposited on an aluminum substrate at $T < 20 \text{ K}$, as well as the double-peaked spectrum of crystalline phase CH_3OH formed by warming amorphous ice to 130 K followed by recoiling to $T < 20 \text{ K}$. The number of peaks and relative intensities of the $\text{CH}_3\text{OH}/\text{silicate}$ spectrum correspond closely to the spectrum of crystalline CH_3OH . The two most intense peaks of the $\text{CH}_3\text{OH}/\text{silicate}$ ice occur at 3297 cm^{-1} and 3180 cm^{-1} ; these

⁵ The actual intensity of each amorphous ice deposit has been maintained in Figs. 2b, 3b, and 4b relative to the intensity of each annealed crystalline ice which has been normalized to 1.

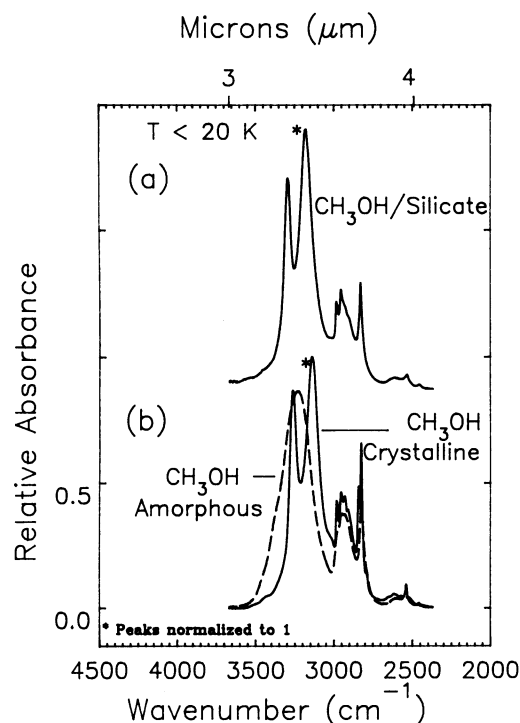


FIG. 3.—Infrared spectra of the O—H stretch region of CH_3OH . CH_3OH deposited directly onto a silicate smoke (a) is compared with spectra of CH_3OH in the amorphous and crystalline phase on an aluminum substrate (b).

are blueshifted more than 30 cm^{-1} from the corresponding 3264 cm^{-1} and 3140 cm^{-1} features in the crystalline phase formed on the aluminum substrate (Fig. 3b). Curve fitting the $\text{CH}_3\text{OH}/\text{silicate}$ spectrum gives a best fit for 100% crystalline.⁶

The mid-infrared spectrum of the ν_2 region of NH_3 near $10\text{ }\mu\text{m}$ is shown in Figure 4. Figure 4a is the spectrum of the $\text{NH}_3/\text{silicate}$. This spectrum is compared with Figure 4b showing the single broad band of amorphous NH_3 deposited on an aluminum substrate at $T < 20\text{ K}$. This deposit was annealed by warming it to near 110 K and then returning to $T < 20\text{ K}$, resulting in the development of two overlapping peaks at 1097 cm^{-1} ($9.1\text{ }\mu\text{m}$) and 1069 cm^{-1} ($9.4\text{ }\mu\text{m}$); most likely these are related to the metastable phase of NH_3 (Sill, Fink, & Ferraro 1980). Complete annealing of this metastable phase to produce a pure crystalline phase was never accomplished before the sample was lost due to rapid sublimation. A spectrum typical of cubic crystalline NH_3 (also shown in Fig. 4b) was obtained by depositing NH_3 on an aluminum substrate at 88 K and then cooling to $T < 20\text{ K}$. The single-peaked spectrum of $\text{NH}_3/\text{silicate}$ has a FWHM = 13 cm^{-1} which is comparable to cubic NH_3 (FWHM = 14 cm^{-1}); in contrast, amorphous NH_3 has a FWHM = 65 cm^{-1} . The peak of the $\text{NH}_3/\text{silicate}$ ice occurs at 1065 cm^{-1} ($9.4\text{ }\mu\text{m}$); it is blueshifted from the 1052 cm^{-1} ($9.5\text{ }\mu\text{m}$) peak of cubic crystalline NH_3 on aluminum. Curve fitting $\text{NH}_3/\text{silicate}$ spectra was not straightforward and will require further examination.

Our laboratory results demonstrate that the formation of predominantly crystalline phase ice occurs during direct

⁶ Lorentzian curves were fitted to the features of pure amorphous and pure crystalline CH_3OH on aluminum. These template curves were fitted to the $\text{CH}_3\text{OH}/\text{silicate}$ spectra. The percent crystalline, for example, was assigned as the fraction of the total peak area of the $\text{CH}_3\text{OH}/\text{silicate}$ represented by the area of the pure crystalline template.

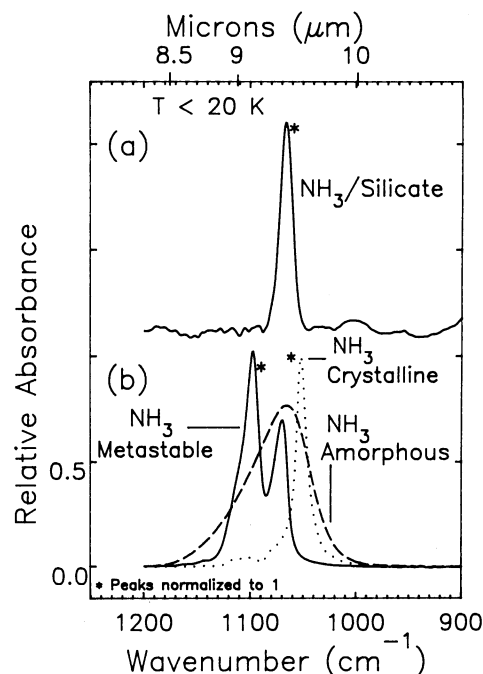


FIG. 4.—Infrared spectra of the ν_2 region of NH_3 . The $\text{NH}_3/\text{silicate}$ spectrum (a) is compared with spectra of NH_3 deposited on an aluminum substrate in the amorphous phase and after annealing that ice to 110 K forming a metastable phase (b). The single peak of cubic crystalline NH_3 (b) was formed by deposition at 88 K .

deposit of H_2O , CH_3OH , or NH_3 at $T < 20\text{ K}$ on amorphous silicate smoke substrates. Some intersample variations occur with silicate smokes prepared at different times (i.e., there is variation in the $10/20\text{ }\mu\text{m}$ ratio and the strength of the $11.4\text{ }\mu\text{m}$ feature), but all amorphous silicate substrates resulted in the low-temperature crystallization (LTC) of condensed ices.

The LTC effect was *not* observed when the ice was formed either on a loose powder made from grains ($3\text{--}100\text{ }\mu\text{m}$ in size) ground from bulk materials (e.g., Si, SiO , SiO_2), or on Si_2O_3 smoke scraped from the inside of our laboratory nucleation chamber. Electron microscope images showed that the scraped off Si_2O_3 had a clump size near several microns. These results suggest that the size of the grains may be an important variable.

It is possible that the LTC occurs due to molecular interactions between the condensing gas and reactive silicate surface sites. Silicate smokes are thought to be a disordered network structure with numerous imperfections and dangling bonds (our preliminary EPR measurements show the presence of unpaired electrons). The hypothesis that active sites (perhaps oxygen vacancy defect sites) may facilitate crystallization is supported by the observation that a lower percent crystalline ice/silicate component formed on smoke substrates partly oxidized by heating to 325°C in air (reducing the number of defect sites). It seems unlikely that any surface reactivity responsible for the LTC would extend beyond an ice layer, yet we find that a second layer of ice is also crystalline in phase. This raises the question of whether the LTC effect is connected to the silicate's low thermal conductivity (TC) or whether some of the active sites were left exposed and in turn facilitated the LTC in the second ice layer.

We have completed a variety of preliminary experiments to examine the possibility that the LTC of ice results from a large

thermal gradient within the silicate smoke. A summary of results are as follows:

1. LTC results on all similarly oxidized silicates regardless of smoke thickness with essentially the same percentage of crystalline component.

2. CO and CH₄ condense on smokes, and CH₄ condenses as a second layer on ultrathin amorphous and on a crystalline CH₃OH/silicate. As temperature probes, CO and CH₄ deposits imply temperatures below 50 K.

3. The temperature-dependent vaporization of ices from ice/silicate smokes appears to be the same as ice films from aluminum substrates.

These results are supported by the following calculations: We assumed that TC for a silicate smoke was $22 \mu\text{W cm}^{-1} \text{K}^{-1}$, the measured value for Cab-O-Sil® (Cabot Corporation 1990) at 100 K (Kuhn et al. 1960). Cab-O-Sil is fumed, amorphous SiO₂, with a porosity and grain size similar to our smokes. The estimated heat flux from the 300 K surfaces seen by the silicate is ~ 100 times less than the heat flux conducted through a 0.5 mm smoke layer at 120 K. Therefore, the surface temperature of a smoke on a 20 K substrate would remain too cold to crystallize ices during direct deposit. The heat of condensation released during deposition was estimated to be an insignificant heat input using the deposition rates typical of these experiments. It has been reported that the TC of slowly deposited

H₂O at 135 K is $4.5 \mu\text{W cm}^{-1} \text{K}^{-1}$ (Sack 1992), a value about one-fifth the TC of Cab-O-Sil. Even if the ice/silicate TC drops by one-fifth after coating with ice, the heat conducted is still estimated to be an order of magnitude above the incoming heat flux.

These experimental results impact ideas concerning the nature of ices in both cometary and interstellar environments. The hypothesis that most ices are accreted in the amorphous phase is central to theories proposing a relationship between cometary outbursts and the exothermic amorphous-to-crystalline phase change of an outer ice layer, and to the idea that volatile species are trapped directly in amorphous deposits and in any clathrate structures formed during warming. The accretion of amorphous phase water ice is the basis for deducing differences in interstellar cloud environments, particularly the temperatures of such clouds. Changes in the 3.1 μm water band have been interpreted in terms of cloud evolution (Graham & Chen 1991; Pendleton, Tielens, & Werner 1990).

The assumption that amorphous phase deposits routinely form on grains at $T < 80$ K needs to be reexamined in light of our laboratory results. We have considered different possibilities for the mechanisms responsible for the LTC, but there are a large number of parameters. Studies are underway to analyze in detail the composition and morphology of the silicate smokes and the ice/silicate mixtures. However, the astrophysical implications of these results remain unchanged regardless of the mechanism.

REFERENCES

- Bertie, J. E., Labbé, H. J., & Whalley, E. 1969, *J. Chem. Phys.*, 10, 4501
 Boice, D. C., Naegeli, D. W., & Hubner, W. F. 1989, in *Proc. of an Internat. Workshop on Phys. and Mech. of Cometary Materials* ed. J. Hunt & T. D. Guyenne (ESA SP-302), 83
 Bregman, J. D., Campins, H., Witteborn, F. C., Wooden, D. H., Rank, D. M., Allamandola, L. J., Cohen, M., & Tielens, A. G. G. M. 1987, *A&A*, 187, 616
 Cabot Corporation 1990, private communication
 Donn, B. 1991, in *Comets in the Post-Halley Era*, ed. R. L. Newburn, Jr., M. Neugebauer, & J. Rahe (Dordrecht: Kluwer), 335
 Graham, J. A., & Chen, W. P. 1991, *AJ*, 102, 1405
 Greenberg, J. M. 1982, in *Comets*, ed. L. Wilkening (Tucson: Univ. of Arizona Press), 131
 Moore, M. H., & Hudson, R. L. 1992, *ApJ*, 401, 353
 Morrow, B. A., & Cody, I. A. 1976, *J. Phys. Chem.*, 80, 1995
 Narten, A. H., Venkatesh, C. G., & Rice, S. A. 1976, *J. Chem. Phys.*, 64, 1106
 Nelson, R., Thiemens, M., Nuth, J., & Donn, B. 1989, *Proc. Lunar Planet. Sci. Conf.*, 19, 559
 Nuth, J. A., III, & Donn, B. 1982, *ApJ*, 257, L103
 Nuth, J. A., III, & Hecht, J. H. 1990, *Ap&SS*, 163, 79
 Pendleton, Y. J., Tielens, A. G. G. M., & Werner, M. W. 1990, *ApJ*, 347, 107
 Rietmeijer, F., & Nuth, J. A., III, 1991, *Proc. Lunar Planet. Sci. Conf.*, 21, 591
 Rietmeijer, F. J. M., Nuth, J. A., III, & Mackinnon, I. D. R. 1986, *Icarus*, 66, 211
 Sack, N. J. 1992, Ph.D. thesis, Univ. of Virginia
 Sill, G., Fink, U., & Ferraro, J. T. 1980, *J. Opt. Soc. Am.*, 70, 724
 Smith, R. G., Selgren, K., & Tokunaga, A. T. 1989, *ApJ*, 344, 413
 Zhao, N. S. 1990, Ph.D. thesis, Univ. Leiden